Antonio Soria-Verdugo[1], Elke Goos[2], Jorge Arrieta-Sanagustín[3], Nestor García-Hernando[1], *Modeling of the pyrolysis of biomass under parabolic and exponential temperature increases using the Distributed Activation Energy Model*, Energy Conversion and Management, Volume 118, 15 June 2016, Pages 223–230.

[1] Carlos III University of Madrid (Spain), Energy Systems Engineering Group, Thermal and Fluids Engineering Department, Avda. de la Universidad 30, 28911 Leganés, Madrid, Spain

[2] Deutsches Zentrum für Luft- und Raumfahrt e.V. (DLR, German Aerospace Center), Institute of Combustion Technology, Pfaffenwaldring 38-40, 70569 Stuttgart, Germany

[3] Instituto Mediterráneo de Estudios Avanzados, IMEDEA, UIB-CSIC, C/ Miguel Marqués 21, 07190 Esporles, Spain

http://dx.doi.org/10.1016/j.enconman.2016.04.003

Modeling of the pyrolysis of biomass under parabolic and exponential temperature increases using the Distributed Activation Energy Model

Antonio Soria-Verdugo[a]*, Elke Goos[b], Jorge Arrieta-Sanagustín[c], Nestor García-Hernando[a]

[a] Carlos III University of Madrid (Spain), Energy Systems Engineering Group, Thermal and Fluids Engineering Department. Avda. de la Universidad 30, 28911 Leganés (Madrid, Spain)

[b] Deutsches Zentrum für Luft- und Raumfahrt e.V (DLR, German Aerospace Center), Institute of Combustion Technology, Pfaffenwaldring 38-40, 70569 Stuttgart (Germany)

[c] Instituto Mediterráneo de Estudios Avanzados, IMEDEA, UIB-CSIC, C/ Miguel Marqués 21, 07190, Esporles (Spain)

* corresponding author: asoria@ing.uc3m.es Tel: +34916248884. Fax: +34916249430.

Abstract

A modification of the simplified Distributed Activation Energy Model is proposed to simulate the pyrolysis of biomass under parabolic and exponential temperature increases. The pyrolysis of pine wood, olive kernel, thistle flower and corncob was experimentally studied in a TGA Q500 thermogravimetric analyzer. The results of the measurements of nine different parabolic and exponential temperature increases for each sample were employed to validate the models proposed. The deviation between the experimental TGA measurements and the estimation of the reacted fraction during the pyrolysis of the four samples under parabolic and exponential temperature increases was lower than 5 ºC for all the cases studied. The models derived in this work to describe the pyrolysis of biomass with parabolic and exponential temperature increases were found to be in good agreement with the experiments conducted in a thermogravimetric analyzer.

***Keywords*:** Distributed Activation Energy Model (DAEM), Biomass pyrolysis, Thermal Gravimetric Analysis (TGA), Parabolic temperature profile, Exponential temperature profile.

Nomenclature:

b	Constant for the parabolic temperature profile [ºC min^{-2}].
c	Constant for the exponential temperature profile [min^{-1}].
c_0	Constant for the exponential temperature profile [ºC].
E_a	Activation energy [kJ mol^{-1}].
E_0	Average value of the activation energy [kJ mol^{-1}].
k_0	Pre-exponential factor [s^{-1}].
R	Universal gas constant [J $mol^{-1}K^{-1}$].
t	Time [s].
T	Temperature over the initial pyrolysis temperature [ºC].
T'	Temperature [ºC].
V	Volatile mass loss [%].
V^*	Volatile mass content [%].

V/V^* Reacted fraction [%].

ϕ_{exp} Value of the ϕ-function for the exponential temperature profile [-].

ϕ_{par} Value of the ϕ-function for the parabolic temperature profile [-].

σ Standard deviation of the activation energy [kJ mol^{-1}].

1. Introduction

Fossil fuels such as oil, natural gas and coal are the most commonly used fuels, corresponding to around 80% of the total primary energy used in the world. This is causing both a pollution problem and international conflicts related to energy security [1]. Biomass is a promising fuel to substitute fossil fuels, due to its renewable nature which comes from its capability of utilizing the carbon dioxide emitted during the biomass conversion to grow the next generation of biomass. The use of biomass-derived fuels has been steadily increasing lately, corresponding currently to more than 14% of the total primary energy consumption in the world [2]. Biomass can be employed for power generation directly in a combustor [3] or to produce desirable products such as liquid biofuels [4], synthesis gas [5], and charcoal [6]. The pyrolysis process is a relevant sub-process in the thermo-chemical conversion of biomass particles in industrial applications, where typically larger particle sizes are employed and thus the reaction inside such particles occurs in absence of oxygen [7].

The kinetics of the biomass pyrolysis can be described based on the activation energy, E_a, and the pre-exponential factor, k_0, of the fuel. There are several different models available in the literature to characterize the pyrolysis process, such as the single step model [8], the two parallel reaction model [9], the three pseudo-components model [10], the sectional approach model [11], and the Distributed Activation Energy Model (DAEM). Vand [12] developed originally the Distributed Activation Energy Model, and Miura [13] and Miura and Maki [14] simplified the mathematical process to obtain the activation energy and pre-exponential factor of the fuel from several thermogravimetric analysis (TGA) curves, obtained at different linear heating rates. The method has been widely used to describe the pyrolysis of a numerous variety of samples, such as coal [14-16], charcoal [17], oil shale [18], polymers [19], solid waste [20, 21], sewage sludge [22], and biomass [22-35]. DAEM has also been employed by Xiong et al. [36] in combination with CFD simulations to describe fast pyrolysis of biomass in fluidized beds obtaining accurate results. This process was analyzed in detail by these authors in [37] and [38].

The main parameters to describe the kinetics of the pyrolysis process, i.e. the activation energy and pre-exponential factor, can be obtained by applying the simplified Distributed Activation Energy Model proposed by Miura and Maki [14] to TGA curves obtained at different linear heating rates. The activation energy and pre-exponential factor can then be employed to model the pyrolysis process occurring at higher heating

rates. Nevertheless, the model is capable of describing the pyrolysis process only under linear temperature increases, which is a significant limitation since the temperature increase in industrial reactors could be faster than linear increase. For instance, the temperature increase of a biomass particle injected in a furnace with a higher homogeneous temperature, such as a fluidized bed, would be exponential, provided that the Biot number of the particle is low. In fact, for low Biot numbers ($Bi < 0.1$), the Lumped Capacitance Method can be employed to determine the temperature of the biomass particle, obtaining an exponential increase of this temperature with time. Exponential heating rates have been employed to analyze the devolatilization of biomass particles in fluidized beds by Saastamoinen [39].

In this work, the simplified Distributed Activation Energy Model proposed by Miura and Maki [14] is modified to describe the pyrolysis process of biomass occurring under parabolic and exponential temperature increases. The selection of the model proposed by Miura and Maki [14] was based on the simplicity of this model to obtain the parameters that describe the pyrolysis kinetics. The mathematical procedure followed by the Miura and Maki [14] model permits to consider parabolic and exponential temperature icreases, which is the focus of our work, without the need of new assumptions. The models derived in this work for parabolic and exponential temperature profiles are validated with measurements of the pyrolysis of four different biomass species (pine wood, olive kernel, thistle flower and corncob) performed in a thermogravimetric analyzer under nine different parabolic and exponential temperature increases. The comparison of the estimations of the models and the experimental data for the nine parabolic and exponential temperature increases of the four biomass species, resulted in temperature deviations lower than 5 ºC for all the cases analyzed.

2. Mathematical model

The Distributed Activation Energy Model was proposed by Vand [12] and, since then, it has been widely used to describe the pyrolysis process of different fuels. DAEM assumes the existence of an infinite number of parallel first order chemical reactions, with a reaction velocity described by the Arrhenius kinetics equation. The reacted fraction, V/V*, can be determined as:

$$1-\frac{V}{V^*}=\int_0^{\infty}\exp\left(-k_0\int_0^t e^{-E/RT}dt\right)f(E)dE \qquad (1)$$

The exponential function in Eq. (1) is the ϕ function:

$$\phi(E,T)=\exp\left(-k_0\int_0^t e^{-E/RT}dt\right) \qquad (2)$$

This ϕ function is typically assumed to be a step function at a value of $E = E_a$, and thus Eq. (1) can be simplified as:

$$\frac{V}{V^*} = \int_0^{E_a} f\left(E_a\right) dE_a \tag{3}$$

2.1. Arrhenius equation for a parabolic temperature profile

Considering a parabolic increase of temperature with time, the ϕ function can be written as:

$$T = b \cdot t^2 \rightarrow \phi(E,T) = \exp\left(-\frac{k_0}{2\sqrt{b}} \int_0^T \frac{e^{-E/RT}}{\sqrt{T}} dT \right) \tag{4}$$

The ϕ function describe in Eq. (4) can be approximated to:

$$\phi(E,T) \cong \exp\left(-\frac{k_0 R T^{1.5}}{2\sqrt{b}E} e^{-E/RT} \right) \tag{5}$$

The value of the activation energy, E_a, is typically selected to satisfy $\phi(E_a,T) = 0.58$, a value found by Miura [13] to obtain a proper approximation for several combinations of k_0 and $f(E)$ when operating with linear temperature profiles. Nevertheless, for a parabolic temperature profile, the value of the ϕ function, $\phi(E_a,T) = \phi_{par}$, to determine the activation energy, E_a, might be different. Knowing this value of the ϕ function, a relation between E_a, b, T, and k_0 can be established:

$$-\ln(\phi_{par}) \frac{2\sqrt{b}E_a}{k_0 R T^{1.5}} = e^{-E_a/RT} \tag{6}$$

Taking the natural logarithm to both sides of Eq. (6) and rearranging terms, the Arrhenius equation for a parabolic temperature profile is obtained.

$$\ln\left(\frac{\sqrt{b}}{T^{1.5}}\right) = \ln\left(\frac{k_0 R}{2E_a}\right) - \ln\left[-\ln\left(\phi_{par}\right)\right] - \frac{E_a}{R}\frac{1}{T} \tag{7}$$

2.2. Arrhenius equation for an exponential temperature profile

The ϕ function for an exponential temperature increase is:

$$T = c_0 \cdot e^{c \cdot t} \rightarrow \phi(E,T) = \exp\left(-\frac{k_0}{c} \int_0^T \frac{e^{-E/RT}}{T} dT \right) \tag{8}$$

The value of the ϕ function for an exponential temperature profile, shown in Eq. (8), can be approximated to:

$$\phi(E,T) \cong \exp\left(-\frac{k_0 R T}{cE} e^{-E/RT} \right) \tag{9}$$

For an exponential increase of temperature with time, the value of the ϕ function, $\phi(E_a,T) = \phi_{exp}$, to determine the activation energy, E_a, should be also determined, so that a relation between E_a, c, T, and k_0 can be written in the form:

$$-\ln(\phi_{\exp})\frac{cE_a}{k_0 RT} = e^{-E_a/RT} \tag{10}$$

Taking the natural logarithm to both sides of Eq. (10) and rearranging terms, the Arrhenius equation for an exponential temperature profile is obtained.

$$\ln\left(\frac{c}{T}\right) = \ln\left(\frac{k_0 R}{E_a}\right) - \ln\left[-\ln\left(\phi_{exp}\right)\right] - \frac{E_a}{R}\frac{1}{T} \tag{11}$$

The Arrhenius equation for a parabolic temperature profile, Eq. (7), and for an exponential temperature profile, Eq. (11), can be employed to determine the temperature at which the devolatilization of a fuel, with activation energy E_a and pre-exponential factor k_0, occurs. Nevertheless, a representative value of the ϕ function, $\phi(E_a,T) = \phi_{par}$ and $\phi(E_a,T) = \phi_{exp}$, to determine the activation energy, E_a, should be selected.

2.3. Value of the ϕ function for a parabolic and exponential temperature profile

Miura [13] obtained a representative value of $\phi(E_a,T)$ to determine the activation energy, E_a, when using a linear temperature profile. Here, the procedure proposed by Muira [13] will be applied to determine the representative value of $\phi(E_a,T) = \phi_{par}$ and $\phi(E_a,T) = \phi_{exp}$, when operating with a parabolic and an exponential temperature profile respectively. The ϕ function can be simplified as a step function for a value $E = E_a$, which can be obtained equaling the following integrals:

$$\int_0^{\infty} \phi f\left(E\right) dE = \int_{E_a}^{\infty} f\left(E\right) dE \tag{12}$$

A distribution should be assumed for $f(E)$ and k_0 to calculate E_a from Eq. (12), being the Gaussian distribution for $f(E)$ and the uniform distribution for k_0 the most typical assumptions [24], [40]:

$$f\left(E\right) = \frac{1}{\sigma\sqrt{2\pi}}\exp\left[-\frac{\left(E-E_0\right)^2}{2\sigma^2}\right] \tag{13}$$

$$k_0 = cte \tag{14}$$

The average value, E_0, and the standard deviation, σ, of the activation energy and the uniform value of k_0 for four different biomass species (pine wood, olive kernel, thistle flower and corncob) were obtained in our previous work [41] for devolatilization rates between 20% and 70%. The values are shown in Table 1.

Sample	E_0 [kJ mol^{-1}]	σ [kJ mol^{-1}]	k_0 [s^{-1}]
Pine wood	165.0	2.6	$1.57 \cdot 10^{12}$
Olive kernel	162.2	3.2	$4.11 \cdot 10^{12}$
Thistle flower	154.5	1.6	$2.80 \cdot 10^{11}$
Corncob	183.5	5.0	$2.31 \cdot 10^{14}$

Table 1: Characteristic values of the Gaussian distribution of *f(E)* and uniform distribution of k_0 for four different biomass samples (obtained from Soria-Verdugo et al. [41]).

The values shown in Table 1 were employed to build the activation energy function, *f(E)*, for each biomass sample. This function was used to determine the activation energy, E_a, needed to fulfill Eq. (12) for each case. Once the activation energy, E_a, was determined, the values of $\phi(E_a,T) = \phi_{par}$ and $\phi(E_a,T) = \phi_{exp}$ were obtained.

The process to obtain ϕ_{par} is shown graphically in Figure 1 for the pine wood and thistle flower samples. Similar results were obtained for the olive kernel and corncob samples.

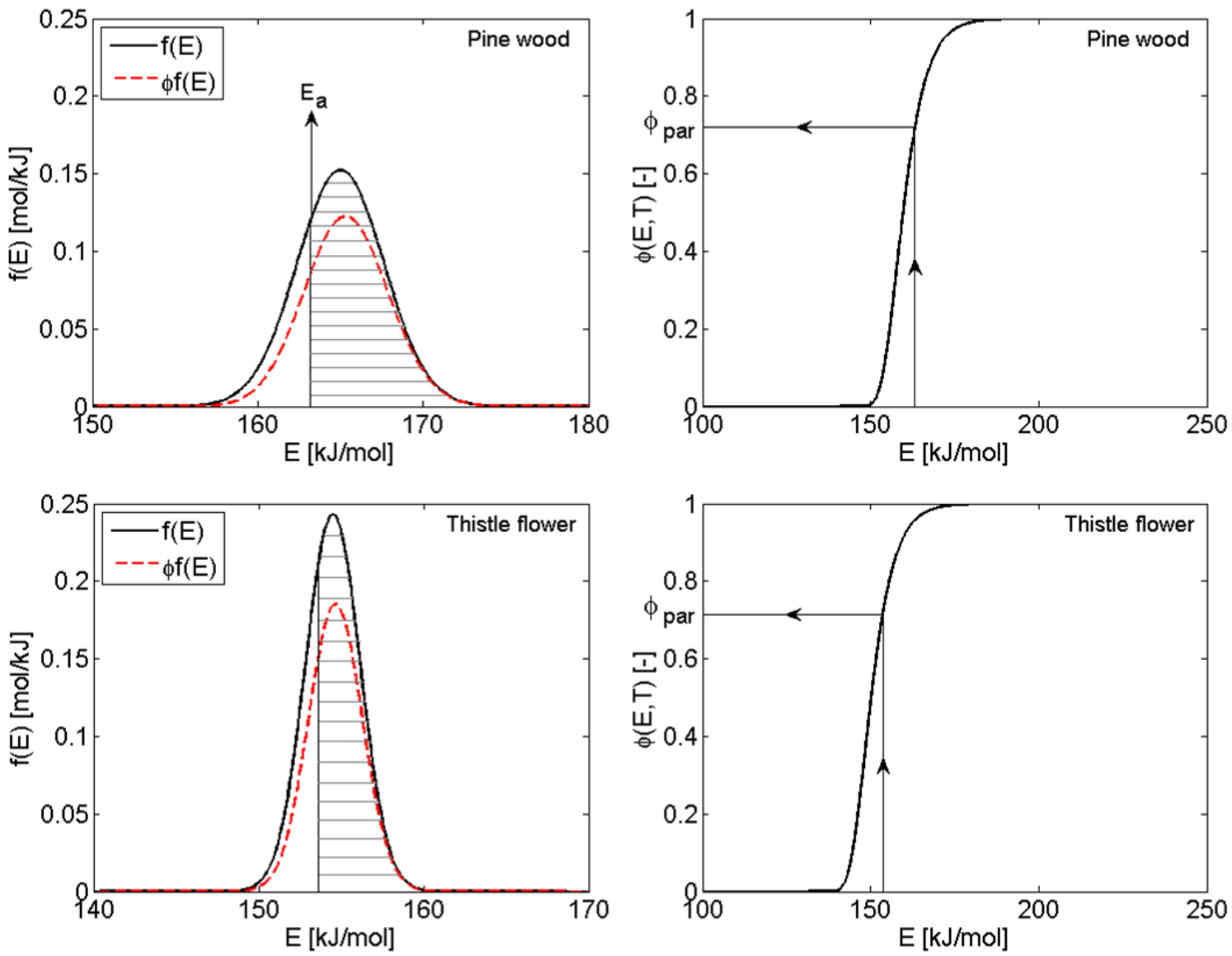

Figure 1: Process to obtain the value of the ϕ function for a parabolic temperature profile (ϕ_{par}).

The values of the ϕ function for a parabolic temperature profile, ϕ_{par}, obtained following the procedure describe in Figure 1 were 0.718 for pine wood, 0.695 for olive kernel, 0.714 for thistle flower and 0.719 for corncob. Therefore, a value of $\phi(E_a,T) = \phi_{par} = 0.71$ is proposed as a representative value. Including this value in Eq. (7), the Arrhenius equation for a parabolic temperature profile is obtained:

$$\ln\left(\frac{\sqrt{b}}{T^{1.5}}\right)=\ln\left(\frac{k_0 R}{2E_a}\right)+1.0715-\frac{E_a}{R}\frac{1}{T} \qquad (15)$$

Following a similar procedure to that described in Figure 1 for the parabolic temperature profile, Figure 2 shows the process to obtain ϕ_{exp} for the pine wood and thistle flower samples, obtaining again similar results for the samples of olive kernel and corncob, which are not represented for simplicity.

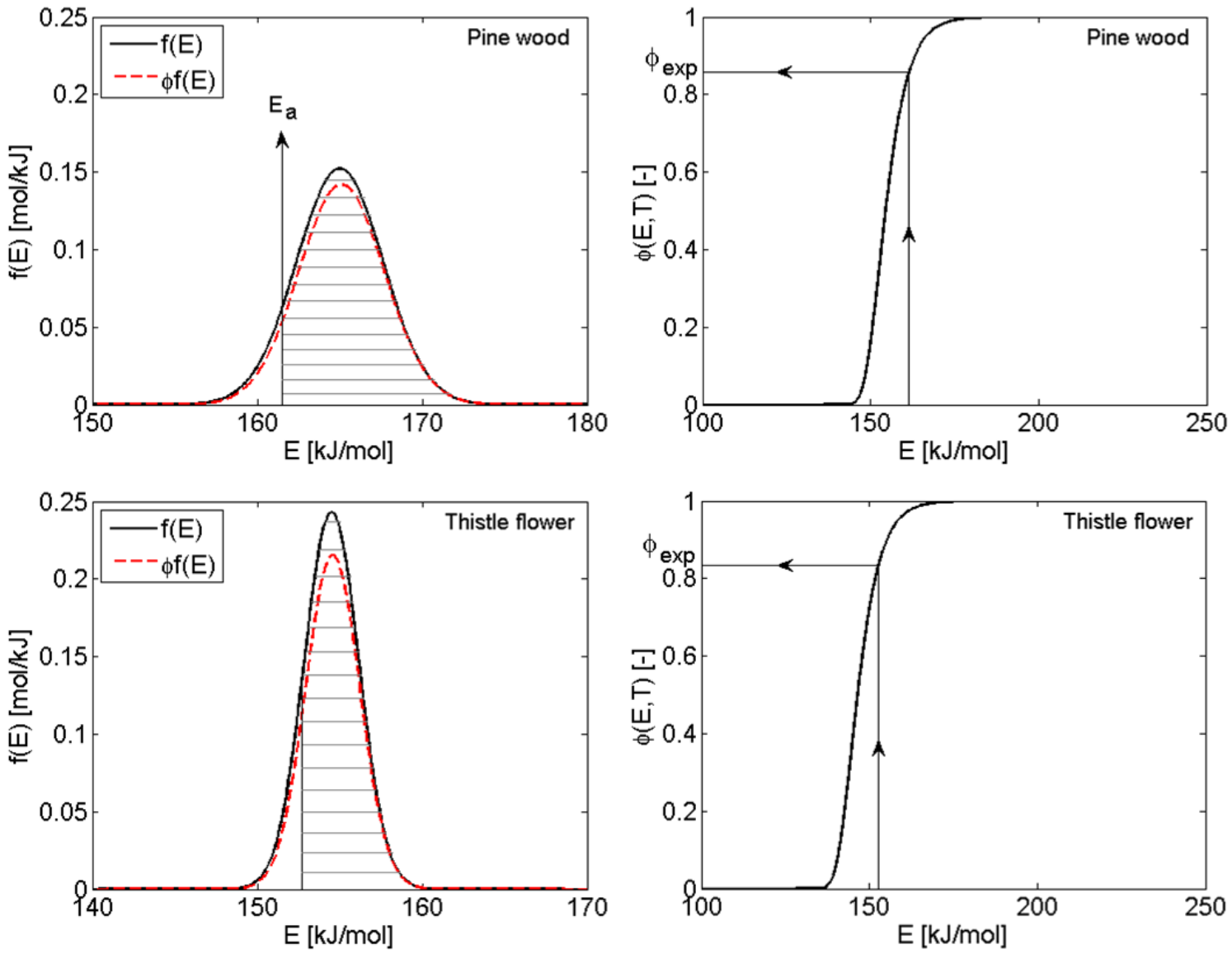

Figure 2: Process to obtain the value of the ϕ function for an exponential temperature profile (ϕ_{exp}).

Following the procedure describe in Figure 2, the values of the ϕ function for an exponential temperature profile, ϕ_{exp}, obtained were 0.852 for pine wood, 0.836 for olive kernel, 0.834 for thistle flower and 0.831 for corncob. Therefore, a representative value of $\phi(E_a,T) = \phi_{exp} = 0.84$ is proposed when analyzing the pyrolysis process of a sample with an exponential temperature increase. Including this value in Eq. (11), the Arrhenius equation for an exponential temperature profile is obtained:

$$\ln\left(\frac{c}{T}\right)=\ln\left(\frac{k_0 R}{E_a}\right)+1.7467-\frac{E_a}{R}\frac{1}{T} \qquad (16)$$

3. Experimental Measurements

The validity of the Arrhenius equations obtained for the parabolic (Eq. 15) and exponential (Eq. 16) temperature increases was analyzed studying the pyrolysis process of four different biomass species using a thermogravimetric analyzer. Thermogravimetric measurements were performed in a TGA Q500 from TA

Instrument under an inert atmosphere, supplying the furnace with a nitrogen flow rate of 60 ml/min. Four different biomass species were tested: pine wood, olive kernel, thistle flower and corncob. The different biomass species analyzed were shredded and sieved. The mass of the samples employed in the TGA tests was 10±0.5 mg, with a particle size lower than 100 μm to avoid heat transfer effects inside the sample, according to the studies of Hu et al. [23] and Mani et al. [42]. A complete characterization of the biomass samples studied was carried out prior to the tests, including a proximate analysis and an ultimate analysis. The proximate analysis was conducted in the TGA Q500 from TA Instrument using an atmosphere of nitrogen for the determination of the humidity (at a temperature of 105 ºC) and the volatile matter content (at a temperature of 900 ºC), whereas the ash content was determined as the mass remaining after a test using an atmosphere of oxygen at a temperature of 550 ºC. The ultimate analysis was performed in a LECO TruSpec CHN Macro and TruSpec S analyzer, capable of measuring the content in carbon, hydrogen, nitrogen and sulfur of the sample. The results of the proximate and ultimate analysis of the different biomass samples are shown in Table 2. The pyrolysis of these four samples under linear temperature increases was studied in a previous work [41], obtaining accurate values for the activation energy, E_a, and the pre-exponential factor, k_0, of each sample.

Proximate analysis				
	Pine wood	Olive kernel	Thistle flower	Corncob
Humidity [%wb]	4.2	4.8	3.9	6.9
Volatile matter [%wb]	78.9	73.3	74.2	80.3
Fixed carbon[a] [%wb]	13.7	19.6	17.7	10.3
Ash content [%wb]	3.2	2.3	4.2	2.5
Elemental analysis				
	Pine wood	Olive kernel	Thistle flower	Corncob
C [%db]	47.1	51.1	44.7	44.8
H [%db]	7.0	6.0	6.0	7.5
N [%db]	0.1	0.9	0.7	1.1
S [%db]	0.1	0.1	0.2	0.2
O[a] [%db]	42.4	39.5	44.0	43.7

Table 2: Results of the proximate analysis and the elemental analysis (wb: wet basis, db: dry basis, [a] obtained by difference).

In this work, the pyrolysis process of pine wood, olive kernel, thistle flower and corncob under parabolic and exponential temperature increases is analyzed. The temperature profile employed during the tests was similar to that employed previously in Soria-Verdugo et al. [41]. First, the temperature was increased from room temperature to 105 ºC and maintained constant during 20 min to dry the sample. Then, the temperature was reduced to 50 ºC to increase linearly from this point to 150 ºC. At 150 ºC the parabolic or exponential temperature increase started, until the temperature reached 700 ºC. Since the thermogravimetic analyzer employed permitted only constant heating rates (i.e. linear temperature increase), the parabolic and exponential temperature increases between 150 ºC and 500 ºC were composed of 25 short linear

temperature increases, guaranteeing that the determination coefficient, R^2, between the measured temperature and the parabolic or exponential fitting was higher than 0.998 for all the cases. Figure 3 shows an example of the measured temperature and the fitting for the parabolic (a) and the exponential (b) temperature profiles, between 150 ºC and 500 ºC where the pyrolysis of the four biomass species occurs [41].

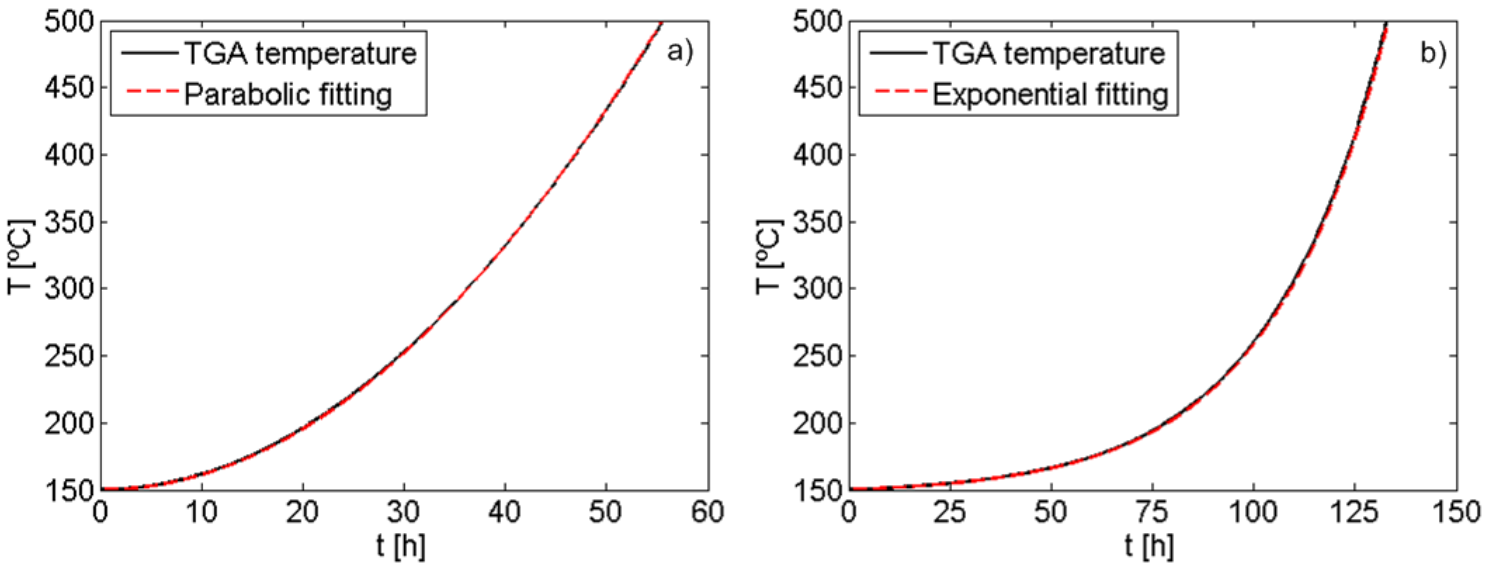

Figure 3: Temperature profiles. a) Parabolic temperature profile (*b = 0.113* ºC min^{-2}). b) Exponential temperature profile (*c = 0.035* min^{-1}).

The parabolic temperature increase during the biomass pyrolysis, between 150 ºC and 500 ºC, follows Eq. (17)

$$T'[^{o}\mathrm{C}] = 150 + b \cdot \left(t[\mathrm{min}]\right)^2 \qquad (17)$$

while the exponential temperature increase follows Eq. (18)

$$T'[^{o}\mathrm{C}] = 146.5 + 3.5 \cdot \exp\left(c \cdot t[\mathrm{min}]\right) \qquad (18)$$

A total of nine different parabolic temperature increases were analyzed, varying the value of *b = 0.050, 0.060, 0.072, 0.090, 0.113, 0.149, 0.203, 0.295, 0.464* ºC min^{-2}. In a similar way, nine different exponential temperature increases were tested, varying the value of *c = 0.023, 0.025, 0.027, 0.031, 0.035, 0.040, 0.047, 0.056, 0.071* min^{-1}.

4. Results and Discussion

The results of the reacted fraction during the pyrolysis process, *V/V**, as a function of temperature, *T'*, for the four biomass samples studied are shown in Figure 4 and Figure 5, for the parabolic and exponential temperature increases respectively. A slight displacement of the pyrolysis process to higher temperatures is observed for faster temperature increases, both for the parabolic (Figure 4) and for the exponential

temperature profiles (Figure 5), as a result of the non-isothermal pyrolysis process as found by Munir et al. [35] and Tonbul et al. [43].

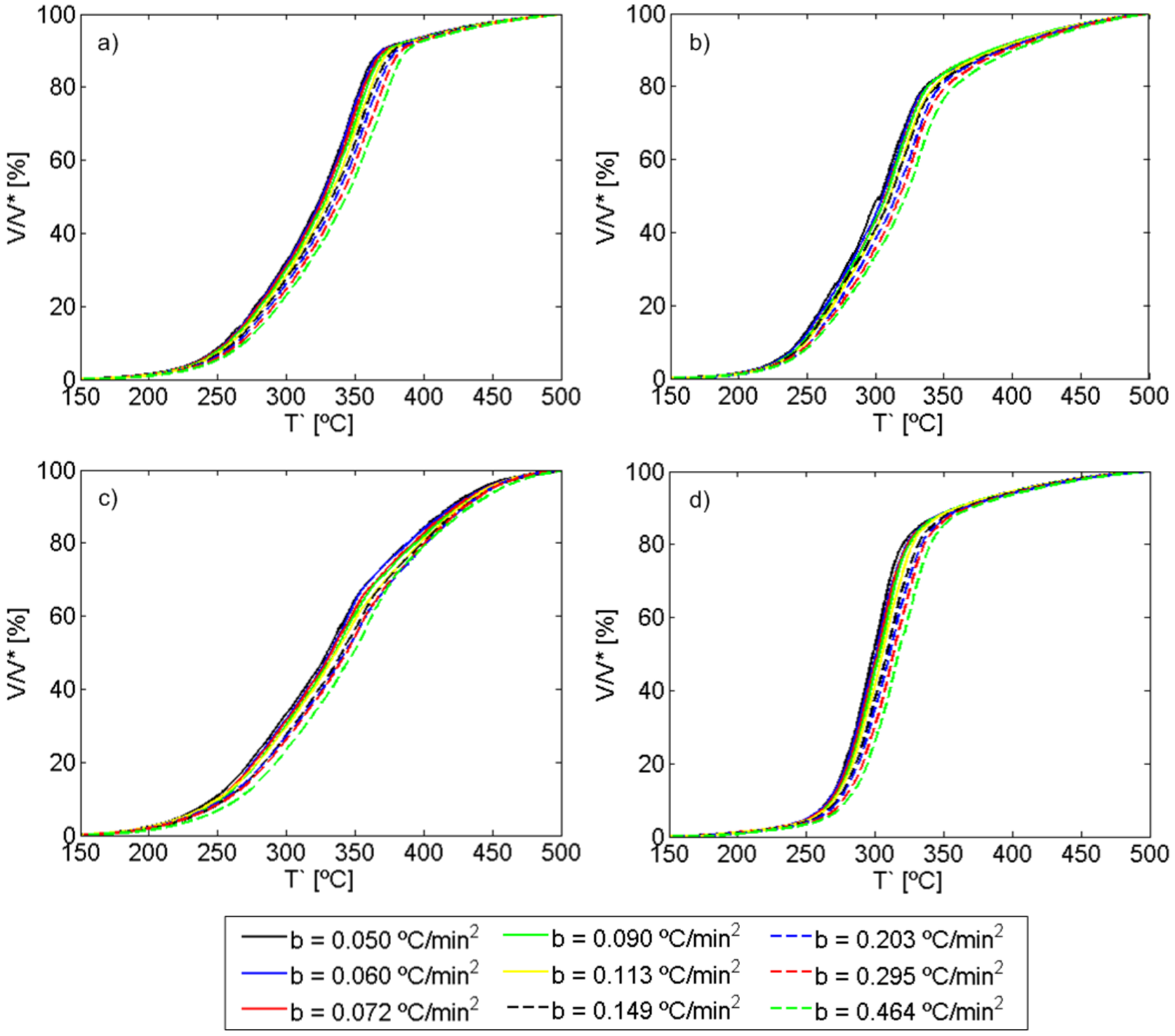

Figure 4: Reacted fraction during the pyrolysis process, *V/V**, as a function of temperature, *T'*, for a parabolic temperature increase. a) Pine wood, b) Olive kernel, c) Thistle flower, d) Corncob.

The differences of the reacted fraction, *V/V**, variation with temperature when this is increased parabolically (Figure 4) or exponentially (Figure 5) are slight. Nevertheless, it should be notice that the differences could be significant when plotting the reacted fraction, *V/V**, as a function of time. The pyrolysis occurs between 250 and 400 ºC for the pine wood (Figure 4 a) and 5 a)) and olive kernel (Figure 4 b) and 5 b)). The pyrolysis temperature range for the thistle flower (Figure 4 c) and 5 c)) is wider, whereas the reacted fraction, *V/V**, of corncob (Figure 4 d) and 5 d)) increases sharply at a temperature around 300 ºC. The measured variation of the reacted fraction, *V/V**, with temperature, *T'*, for the four biomass samples subjected to parabolic and exponential temperature increases, shown respectively in Figures 4 and 5, will be used to test the validity of the Arrhenius equations obtained in Section 2.

The Arrhenius equations for the parabolic (Eq. 15) and the exponential (Eq. 16) temperature profiles can be employed to calculate the temperature, T, for a particular reacted fraction, V/V^*, provided that the activation energy, E_a, and the pre-exponential factor, k_0, of the sample are known. Accurate values of the activation energy, E_a, and the pre-exponential factor, k_0, of the pine wood, olive kernel, thistle flower and corncob were obtained previously in Soria-Verdugo et al. [41], using nine different linear heating rates. The values obtained in Soria-Verdugo et al. [41] for the activation energy and pre-exponential factor of the different samples are shown in Figure 6. These kinetic parameters (E_a and k_0) for the pine sample are in agreement with those of Shen et al. [26] and Poletto et al. [32], the values for the olive kernel sample are similar to those obtained by Aboulkas et al. [45] and Ounas et al. [46], the activation energy and pre-exponential factor of the thistle flower sample are comparable to the values reported by Damartzis et al. [47], and the results obtained for the corncob sample are similar to those of Sonobe and Worasuwannarak [25] and Chen et al. [29].

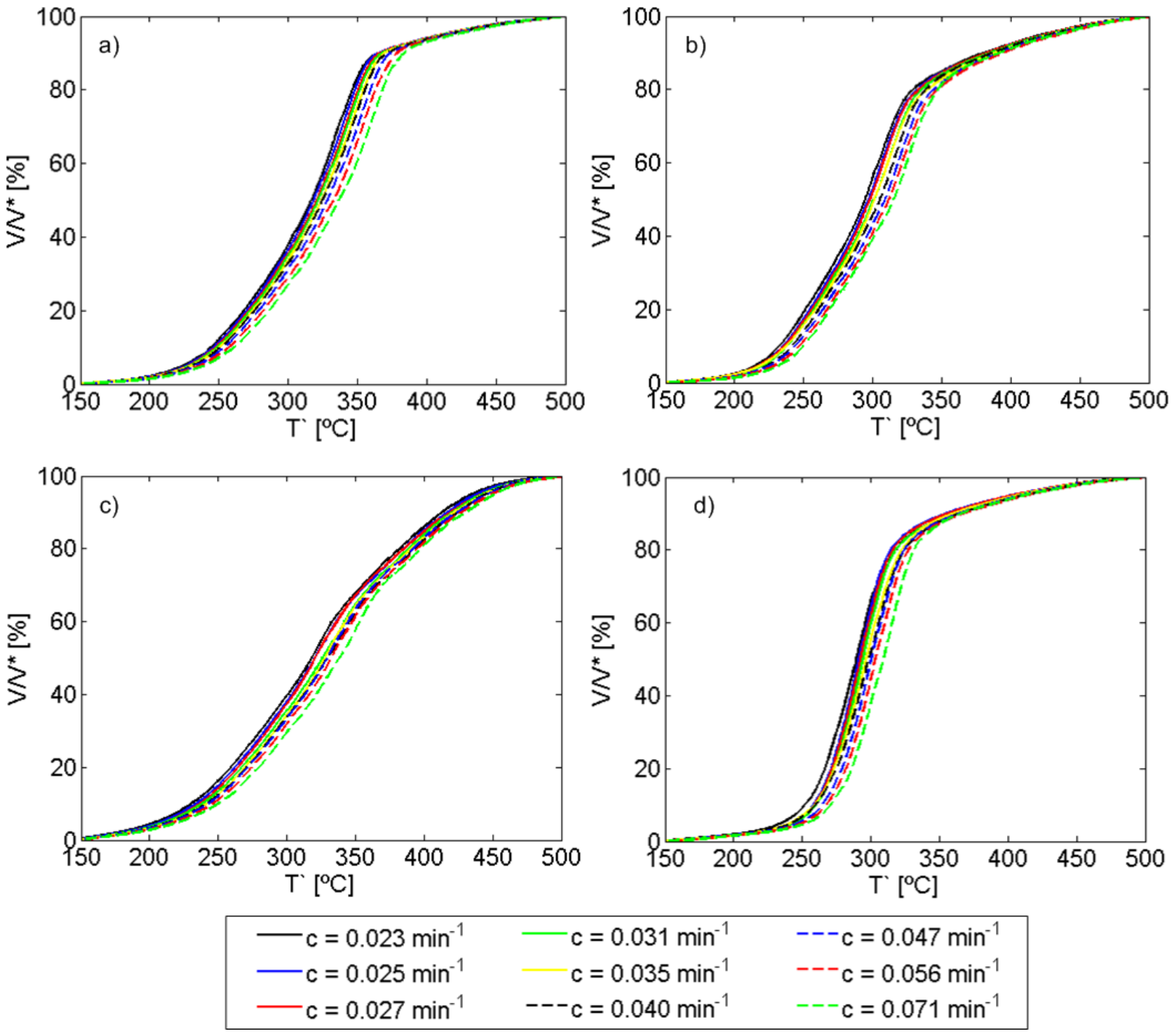

Figure 5: Reacted fraction during the pyrolysis process, V/V^*, as a function of temperature, T', for an exponential temperature increase. a) Pine wood, b) Olive kernel, c) Thistle flower, d) Corncob.

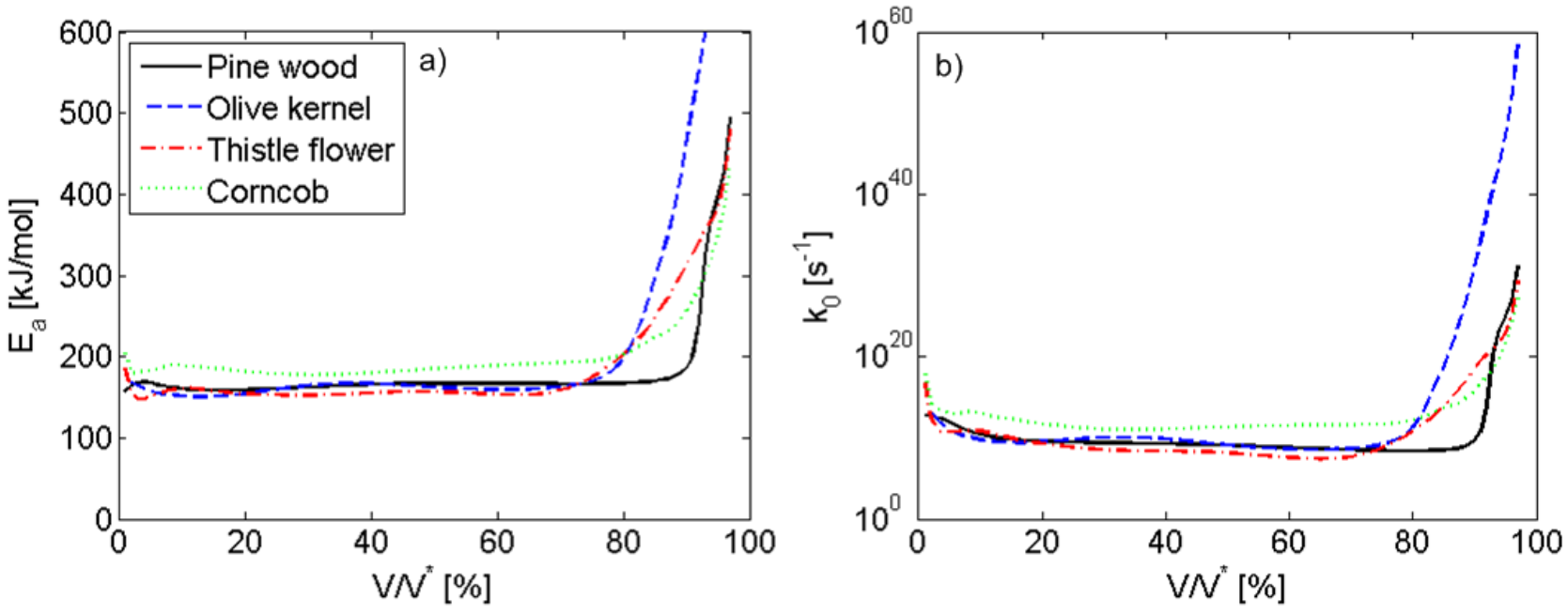

Figure 6: Activation energy (a) and pre-exponential factor (b) of the four biomass species studied, obtained from nine different linear heating rate TGA curves in Soria-Verdugo et al. [41].

The values of the activation energy, E_a, and pre-exponential factor, k_0, as a function of the reacted fraction, *V/V**, shown in Figure 6 can be included in the Arrhenius equations for a parabolic temperature profile (Eq. 15) or for an exponential temperature profile (Eq. 16). Solving the Arrhenius equations for a particular value of *b* (parabolic temperature increase) or *c* (exponential temperature increase) employing a Newton-Raphson method, the temperature, *T*, at which a particular value of the reacted fraction, *V/V**, occurred was calculated, and thus the relation of *V/V** and *T* was numerically derived. The relation of *V/V** and *T* obtained solving the Arrhenius equation for the parabolic temperature increase (Eq. 15) was compared to the measured values presented in Figure 4, and the estimated variation of *V/V** and *T* obtained solving the Arrhenius equation for the exponential temperature increase (Eq. 16) was compared to the measured values shown in Figure 5. The deviation between the temperature estimated by the Arrhenius equations and the measured temperature is plotted in Figure 7 for all the biomass species, using both the parabolic (a) and exponential (b) temperature increases. Figure 7 shows only one case for the parabolic ($b = 0.113$ ºC min^{-2}) and the exponential ($c = 0.035$ min^{-1}) temperature profiles, nevertheless the deviation is lower than 5 ºC for all the cases measured, which seems to be acceptable since this deviation is similar to the differences in the reactor temperature obtained by Park et al. [44] during the pyrolysis process of biomass in a fluidized bed, a system characterized by an homogeneous temperature. The deviation between the experimental results and the curves obtained using directly the model proposed by Miura and Maki [14] with a linear temperature increase, with the same initial and final point than the parabolic and exponential increases, was more than five times larger than those obtained employing the Arrhenius equations for the parabolic and exponential temperature profiles. Therefore, the Arrhenius equations for the parabolic (Eq. 15) and exponential (Eq. 16) temperature increases seem to describe accurately the pyrolysis process of biomass subjected to these

temperature profiles. The model could be also employed for higher heating rates provided that the heat and mass transfer effects inside the sample are negligible.

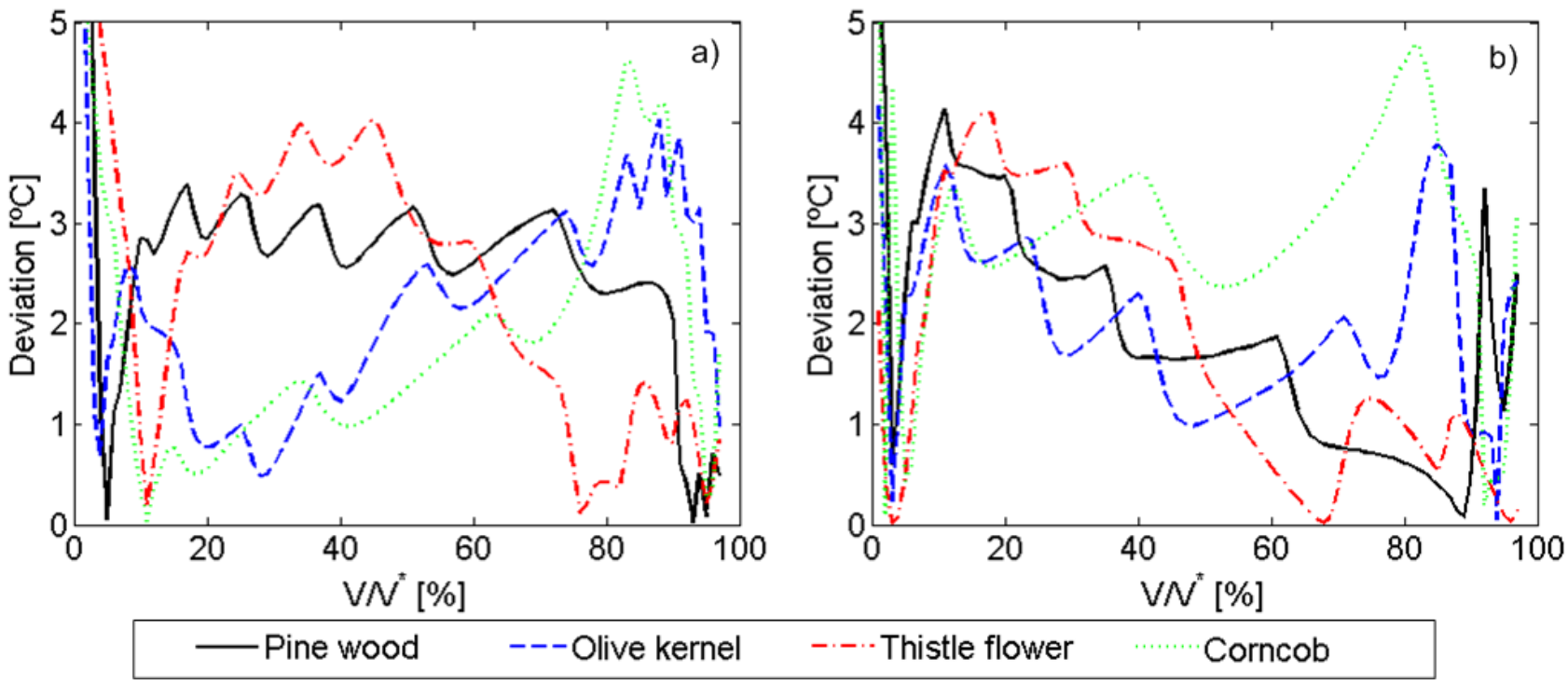

Figure 7: Deviation between the temperature estimated by the Arrhenius equations and the temperature measured in TGA. a) Parabolic temperature profile ($b = 0.113$ ºC min^{-2}) b) Exponential temperature profile ($c = 0.035$ min^{-1}).

5. Conclusions

The simplified Distributed Activation Energy Model proposed by Miura and Maki [14] was modified to enable the description of the pyrolysis process of solid fuels under parabolic and exponential temperature increases. The pyrolysis process under parabolic and exponential temperature profiles was experimentally characterized in a thermogravimetric analyzer. Nine different parabolic and exponential temperature increases were obtained by a composition of 25 short linear temperature increases, which guarantee a high determination coefficient between the composition of linear increases and the parabolic or exponential temperature increase. Four different biomass samples of pine wood, olive kernel, thistle flower and corncob were subjected to the nine parabolic and exponential temperature profiles in the thermogravimetric analyzer, measuring the reacted fraction as a function of the temperature during the pyrolysis process. The model proposed was validated by the comparison of the reacted fraction predicted by the model and that measured in the TGA, obtaining deviations lower than 5 ºC for the four biomass samples analyzed under the nine different parabolic and exponential temperature profiles. Therefore, the models proposed to describe the pyrolysis of biomass under parabolic and exponential temperature increases were found to estimate accurately the reacted fraction of the fuel as a function of temperature during the pyrolysis process with parabolic and exponential temperature profiles.

Acknowledgments

The authors express their gratitude to the BIOLAB experimental facility and to the “Programa de movilidad de investigadores en centros de investigación extranjeros (Modalidad A)” from the Carlos III University of Madrid (Spain) for the financial support conceded to Antonio Soria for a research stay at the German Aerospace Center DLR (Stuttgart, Germany) during the summer of 2014. The authors also gratefully acknowledge the financial support provided by Fundación Iberdrola under the “VI Programa de Ayudas a la Investigación en Energía y Medioambiente”. Funding by the combustion and gas turbine technology program (EVG), of Deutsches Zentrum für Luft- und Raumfahrt e. V. (DLR), the German Aerospace Center, is gratefully acknowledged by Elke Goos.

References

[1] Song J, Song SJ, Oh S-D, Yoo Y. Evaluation of potential fossil fuel conservation by the renewable heat obligation in Korea. Renew. Energ. 2015; 79, 140-149.

[2] Saxena RC, Adhikari DK, Goyal HB. Biomass-based energy fuel through biochemical routes: A review. Renew. Sust. Energ. Rev. 2009; 13, 167-178.

[3] Saidur R, Abdelaziz EA, Demirbas A, Hossain MS, Mekhilef S. A review on biomass as a fuel for boilers. Renew. Sust. Energ. Rev. 2011; 15, 2262-2289.

[4] Pütün AE, Burcu Uzun B, Apaydin E, Pütün E. Bio-oil from olive oil industry wastes: Pyrolysis of olive residue under different conditions. Fuel Process. Technol. 2005; 87, 25-32.

[5] Kaewluan S, Pipatmanomai S. Potential of synthesis gas production from rubber wood chip gasification in a bubbling fluidised bed gasifier. Energy Convers. Manage. 2011; 52, 75-84.

[6] Prins MJ, Ptasinski KJ, Janssen FJJG. Torrefaction of wood: Part 1 Weight loss kinetics. J. Anal. Appl. Pyrol. 2006; 77, 28-34.

[7] Gómez-Barea A, Leckner B, Villanueva Perales AL, Campoy M. Analytical solutions of sharp interface models with nth order kinetics. Application to char conversion. Chem. Eng. J. 2012; 183, 408-421.

[8] Coats AW, Redfern JP. Kinetic parameters from thermogravimetric data. Nature 1964; 201, 68-69.

[9] Anca-Couce A, Berger A, Zobel N. How to determine consistent biomass pyrolysis kinetics in a parallel reaction scheme. Fuel 2014; 123, 230-240.

[10] Li Z, Zhao W, Meng B, Liu C, Zhu Q, Zhao G. Kinetic study of corn straw pyrolysis: Comparison of two different three-pseudo component models. Bioresource Technol. 2008; 99, 7616-7622.

[11] Lin T, Goos E, Riedel U. A sectional approach for biomass: Modelling the pyrolysis of cellulose. Fuel Process. Technol. 2013; 115, 246-253.

[12] Vand V. A theory of the irreversible electrical resistance changes of metallic films evaporated in vacuum. Proc. Phys. Soc. 1943; 55, 222-246.

[13] Miura K. A new and simple method to estimate f(E) and k_0(E) in the distributed activation energy model from three sets of experimental data. Energ. Fuel. 1995; 9, 302-307.

[14] Miura K, Maki T. A simple method for estimating f(E) and k_0(E) in the distributed activation energy model. Energ. Fuel. 1998; 12, 864-869.

[15] Günes M, Günes SK. Distributed activation energy model parameters of some Turkish coals. Energy Sources Part A - Recovery Utilization and Environmental Effects 2008; 30, 1460-1472.

[16] Li Z. Liu C, Chen Z, Qian J, Zhao W, Zhu Q. Analysis of coals and biomass pyrolysis using the distributed activation energy model. Bioresource Technol. 2009; 100, 948-952.

[17] Várghegyi G, Szabó P, Antal MJ. Kinetics of charcoal devolatilization. Energ. Fuel. 2002; 16, 724-731.

[18] Wang Q, Wang H, Sun B, Bai J, Guan X. Interactions between oil shale and its semi-coke during co-combustion. Fuel 2009; 88, 1520-1529.

[19] Wanjun T, Cunxin W, Donghua C. Kinetic studies on the pyrolysis of chitin and chitosan. Polym. Degrad. Stabil. 2005; 87, 389-394.

[20] Yan JH, Zhu HM, Jiang XG, Chi Y, Cen KF. Analysis of volatile species kinetics during typical medical waste materials pyrolysis using a distributed activation energy model. J. Hazard. Mater. 2009; 162, 646-651.

[21] Bhavanan A, Sastry RC. Kinetic study of solid waste pyrolysis using distributed activation energy model. Bioresource Technol. 2015; 178, 126-131.

[22] Soria-Verdugo A, Garcia-Hernando N, Garcia-Gutierrez LM, Ruiz-Rivas U. Analysis of biomass and sewage sludge devolatilization using the distributed activation energy model. Energy Convers. Manage. 2013; 65, 239-244.

[23] Hu S, Jess A, Xu M. Kinetic study of Chinese biomass slow pyrolysis: Comparison of different kinetic models. Fuel 2007; 86, 2778-2788.

[24] Cai J, Liu R. New distributed activation energy model: Numerical solution and application to pyrolysis kinetics of some types of biomass. Bioresource Technol. 2008; 99, 2795-2799.

[25] Sonobe T, Worasuwannarak N. Kinetic analyses of biomass pyrolysis using the distributed activation energy model. Fuel 2008; 87, 414-421.

[26] Shen DK, Gu S, Jin B, Fang MX. Thermal degradation mechanisms of wood under inert and oxidative environments using DAEM methods. Bioresource Technol. 2011; 102, 2047-2052.

[27] Soria-Verdugo A, Garcia-Gutierrez LM, Blanco-Cano L, Garcia-Hernando N, Ruiz-Rivas U. Evaluating the accuracy of the Distributed Activation Energy Model for biomass devolatilization curves obtained at high heating rates. Energy Convers. Manage. 2014; 86, 1045-1049.

[28] Yang X, Zhang R, Fu J, Geng S, Cheng JJ, Sun Y. Pyrolysis kinetic and product analysis of different microalgal biomass by distributed activation energy model and pyrolysis-gas chromatography-mass spectrometry. Bioresource Technol. 2014; 163, 335-342.

[29] Chen D, Zheng Y, Zhu X. In-depth investigation on the pyrolysis kinetics of raw biomass. Part I: Kinetic analysis for the drying and devolatilization stages. Bioresource Technol. 2013; 131, 40-46.

[30] Fiori L, Valbusa M, Lorenzi D, Fambri L. Modeling of the devolatilization kinetics during pyrolysis of grape residues. Bioresource Technol. 2012; 103, 389-397.

[31] Ma F, Zeng Y, Wang J, Yang Y, Yang X, Zhang X. Thermogravimetric study and kinetic analysis of fungal pretreated corn stover using the distributed activation energy model. Bioresource Technol. 2013; 128, 417-422.

[32] Poletto M, Zattera AJ, Santana RMC. Thermal decomposition of wood: Kinetics and degradation mechanisms. Bioresource Technol. 2012; 126, 7-12.

[33] Guo F, Dong Y, Lu Z, Fan P, Yang S, Dong L. Pyrolysis kinetics of biomass (herb residue) under isothermal condition in a micro fluidized bed. Energy Convers. Manage. 2015; 93, 367-376.

[34] Ceylan S, Kazan D. Pyrolysis kinetics and thermal characteristics of microalge Nanochloropsis oculata and Tetraselmis sp. Bioresource Technol. 2015; 187, 1-5.

[35] Munir S, Daood SS, Nimmo W, Cunliffe AM, Gibbs BM. Thermal analysis and devolatilization kinetics of cotton stalk, sugar cane bagasse and shea meal under nitrogen and air atmospheres. Bioresource Technol. 2009; 100, 1413-1418.

[36] Xiong Q, Zhang J, Xu F, Wiggins G, Stuart Daw C. Coupling DAEM and CFD for simulating biomass fast pyrolysis in fluidized beds. J. Annal. Appl. Pyrol. 2016; 117, 176-181.

[37] Xiong Q, Kong SC, Passalacqua A. Development of a generalized numerical frame work for simulating biomass fast pyrolysis in fluidized-bed reactors. Chem. Eng. Sci. 2013; 99, 305-313.

[38] Xiong Q, Aramideh S, Kong SC. Assessment of devolatilization schemes in predicting product yields of biomass fast pyrolysis. Environ. Prog. & Sustain. Energy 2014; 33, 756-761.

[39] Saastamoinen JJ. Simplified model for the calculation of devolatilization in fluidized beds. Fuel 2006; 85, 2388-2395.

[40] Cai J, Wu W, Liu R. An overview of distributed activation energy model and its application in the pyrolysis of lignocellulosic biomass. Renew. Sust. Energ. Rev. 2014; 36, 236-246.

[41] Soria-Verdugo A, Goos E, Garcia-Hernando N. Effect of the number of TGA curves employed on the biomass pyrolysis kinetics results obtained using the Distributed Activation Energy Model. Fuel Process. Technol. 2015; 134, 360-371.

[42] Mani T, Murugan P, Abedi J, Mahinpey N. Pyrolysis of wheat straw in a thermogravimetric analyzer: effect of particle size and heating rate on devolatilization and estimation of global kinetics. Chem. Eng. Res. Des. 2010; 88, 952-958.

[43] Tonbul Y, Saydut A, Yurdako K, Hamamci C. A kinetic investigation on the pyrolysis of Seguruk asphaltite. J. Therm. Anal. Calorim. 2009; 95, 197-202.

[44] Park HJ, Park YK, Dong JI, Kim JS, Jeon JK, Kim SS, Kim J, Song B, Park J, Lee KJ. Pyrolysis characteristics of Oriental white oak: Kinetic study and fast pyrolysis in a fluidized bed with an improved reaction system. Fuel Process. Technol. 2009; 90, 186-195.

[45] Aboulkas A, El Harfi K, El Bouadili A. Pyrolysis of olive residue/low density polyethylene mixture: Part I Thermogravimetric kinetics. J. Fuel Chem. Technol. 2008; 36(6), 672-678.

[46] Ounas A, Aboulkas A, El Harfi K, Bacaoui A, Yaacoubi A. Pyrolysis of olive residue and sugar cane bagasse: Non-isothermal thermogravimetric kinetic analysis. Bioresource Technol. 2011; 102, 11234-11238.

[47] Damartzis T, Vamvuka D, Sfakiotakis S, Zabaniotou A. Thermal degradation studies and kinetic modeling of cardoon (Cynara cardunculus) pyrolysis using thermogravimetric analysis (TGA). Bioresource Technol. 2011; 102 6230-6238.

List of Figures

List of Tables